Proceedings of the
47th IEEE Conference on Decision and Control
Cancun, Mexico, Dec. 9-11, 2008

Analysis and control of the air system of a turbocharged gasoline engine

Philippe Moulin and Jonathan Chauvin

Abstract— **This paper investigates the modelling and the control of a turbocharged air system of a gasoline engine. The purpose of the work described here is to propose a new control strategy based on an original physical model of the system. Starting from a model described in a previous publication, we analyze the system properties in terms of states of equilibrium, stability, and robustness. This analysis justifies the structure chosen for the innovative control strategy, based on the inversion of the model. This strategy takes input constraints into account and includes an anti windup scheme. Experimental results are proposed on a 4 cylinder turbocharged gasoline engine, along with a comparison between the contribution of the different terms of the control strategy.**

I. Introduction

Decreasing the size of automotive engines seems to be a promising solution to reduce the CO_2 emissions. The purpose is to reduce the volumetric capacity of the engine, and hence improve its efficiency chain via a diminution in friction and pumping losses. This technique is called downsizing. In downsized engines, the lack of power induced by the reduction of air charge capacity can be compensated by the use of turbochargers which become more and more complex. At the same time, the associated control strategies need to be adapted and improved. The primary purpose of this work is to understand the functioning of a turbocharger, and design an appropriate control law.

The standard controllers are composed mostly by linear controller (see [5], [11], [13]). They exhibit some disadvantages linked to the application of linear control techniques to non linear systems : the compromise obtained between performance and robustness is suboptimal on the whole operating range of the system. Neural networks [1] or sliding modes [8] can be also used but are not robust to varying operating conditions. These issues are partly corrected by the use of gain scheduling techniques and the addition of static feed forward terms leading to a high calibration effort. These are based on parameters given by maps which depend on the system state. This approach is compromised with the new technologies whose complexity increases the difficulties encountered.

Applicable models of turbocharged gasoline systems are well documented in [6], [4], [2], [3] or [10]. It consists mainly in a energy balance between the compressor and the turbine. The main difficulty comes from the nonlinear dynamics and the dependency in unmeasured parameters. The introduction of model based structures is considered to improve the standard linear controllers with feed forward. Indeed, it allows a dynamic feedforward and a structured feedback. A novel model-based strategy was proposed in a Diesel engine technology context in [9], [12]. In [7], we use the same model based approach and propose a model and strategy simplification due to the gasoline application. The purpose of this paper is to extend this work with an analysis of the systems properties and the consideration of actuators constraints in the control strategy.

The paper is organized as follows. In Section II, we describe the system. The control objectives are presented in Section III. In Section IV, we present the model of the turbocharger and propose an analysis of the behavior of the system (equilibrium and stability). The control strategy is proposed in Section V. Finally, experimental results are reported in Section VI.

II. System description

The engine considered in this paper is a four cylinder turbocharged gasoline engine. Figure 1 shows the architecture of the system. The fresh air enters in the engine through the compressor which increases the air density. This air is used as a comburant in the cylinder where the combustion occurs, resulting in the production of mechanical torque. The remaining energy contained in the gas in the form of enthalpy exits the system through the turbine. Part of the gas enthalpy is then converted into mechanical power on the turbocharger shaft, whose dynamics are the consequences of the balance between the compressor and turbine energies. Two actuators are available on the air system :

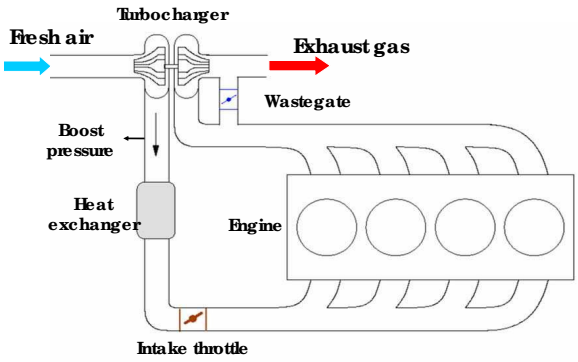

Fig. 1. Engine scheme.

P. Moulin and J. Chauvin are with the engine control team at IFP. Institut Français du Pétrole, 1 et 4 Avenue de Bois Préau, 92852 Rueil Malmaison, France. Corresponding author: Philippe Moulin. philippe.moulin@ifp.fr

- The intake throttle which allows to reach low pressure in the intake manifold
- The wastegate valve. Its function is to divert from the turbine part of the exhaust gas. When this valve is opened, the turbine mass flow and enthalpy are reduced, and so is the energy provided to the shaft.

The sensors available on the system are the following :

- Compressor downstream pressure P_{dc}.
- Compressor upstream pressure and temperature P_{uc} and T_{uc}.
- Engine intake manifold pressure and temperature P_{man} and T_{man}.

III. Control objectives

The main objective of the engine control strategies is to produce a required mechanical torque on the engine shaft. On a gasoline engine running at stoichiometry, this torque is directly linked with the air mass aspirated by the cylinder which in turn depends on the intake manifold air density. The goal of the air path management is therefore to control the intake manifold pressure. The intake throttle allows a fast and direct action on this variable, but is constrained by its upstream pressure at the compressor outlet. The aim of the turbocharger control strategy is therefore to actuate the wastegate in order to follow a compressor downstream pressure set-point. In this case, and contrary to the throttle, the action on the system is indirect : the effect of the wastegate on the compressor depends on the turbocharger dynamics. Indeed, the wastegate acts as a discharge valve on the turbine flow that influences the compressor power through the turbocharger crankshaft. Additionally than following the pressure set-point, the following constraints have to be followed :

- In steady state, the pressure drop through the throttle has to be minimized in order to avoid energy losses. A consequence is that when operating at high loads the throttle will be fully opened.
- The control law has to be robust with respect to environmental conditions variations : the thermodynamic conditions at the boundaries of the system will affect its behavior.
- The speed of the turbocharger shaft has to be maintained below a maximum value.

In order to satisfy the first constraint, the supercharging pressure set-point will be taken equal to the intake manifold pressure set-point. The throttle will then be automatically opened in steady state. For the following of this paper, the engine is considered to be operated under turbocharging. So we consider that the throttle is open, and that $P_{dc} = P_{man}$.

IV. Model analysis

A. Turbocharger modeling

The turbocharger is composed by a turbine driven by the exhaust gas and connected via a common shaft to the compressor, which compresses the air at the engine intake. The rotational speed of the turbocharger shaft N_t can be derived from a power balance between the turbine $\mathcal{P}_t$ and the compressor side $\mathcal{P}_c$

$$\frac{d}{dt}(\frac{1}{2}J_t N_t^2) = \mathcal{P}_t - \mathcal{P}_c$$

where J_t is the inertia of the turbocharger. A nomenclature is presented in Table I. The different elements of the model

Var.	Quantity	Unit
J_t	Turbocharger inertia	
N_t	Turbocharger speed	rad.s$^-$1
$\mathcal{P}_c$	Compressor power	-
$\mathcal{P}_t$	Turbine power	-
P_{uc}	Pressure upstream compressor	Pa
P_{dc}	Pressure downstream compressor	Pa
P_{ut}	Pressure upstream turbine	Pa
P_{dt}	Pressure downstream turbine	Pa
T_{uc}	Ambient temperature	K
T_{dc}	Downstream compressor temperature	K
T_{ut}	Upstream turbine temperature	K
u	Control	-
η_c	Compressor efficiency	-
η_t	Turbine efficiency	-
η_v	Volumetric efficiency	-
Π_c	Compressor pressure ratio	-
Π_t	Turbine pressure ratio	-

TABLE I
Nomenclature.

are presented in [7] which details the different stages that lead to this system of equations. Through modelling efforts and simplifications, the reference system writes

$$\left\{ \begin{array}{rcl} \dot{\Pi}_c &=& \alpha_1 \psi_t(\Pi_t) - \alpha_2 \psi_c(\Pi_c) \\ \Pi_c &=& \alpha_3(\phi_{turb}(\Pi_t) + u S_{wg,max}\phi_{wg}(\Pi_t)) \end{array} \right. \quad (1)$$

where Π_c is the compressor pressure ratio, Π_t is the turbine pressure ratio The functions ψ_c, ψ_t, ϕ_{turb}, ϕ_{wg} are strictly increasing invertible functions, and the $\{\alpha_i\}_{i\in[1,3]}$ are positive and depend on the engine operating conditions

$$\left\{ \begin{array}{rcl} \alpha_1 &=& c_p\sqrt{T_{ut}}P_{dt}\eta_t \frac{2}{J_t a} \\ \alpha_2 &=& \eta_v \Psi N_e C_p T_{uc} \frac{1}{\eta_c}\frac{2}{J_t a} \\ \alpha_3 &=& \frac{P_{dt}}{\sqrt{T_{ut}}(1+\lambda_s)N_e\Psi\eta_v} \end{array} \right.$$

In the following, the words command or actuator are used for the model input u, and Ψ depends on environmental conditions ($\Psi \triangleq \frac{V_{cyl}P_{atm}}{120RT_{int}}$).

B. Trajectories of the system

The simple representation provided by model (1) helps to better understand the system. Since it is particularly interesting to analyze its behavior with respect to engine speed, the coefficients α_i are approximated in the following by an average value at each engine speed. This does not change the macroscopic analysis of the system and simplifies the study. First of all, we write Π_t in function of Π_c and u by inverting the second equation of system (1) which is static, leading to

$$\dot{\Pi}_c = \alpha_1 \Psi_t(\Pi_c, u) - \alpha_2 \psi_c(\Pi_c)$$

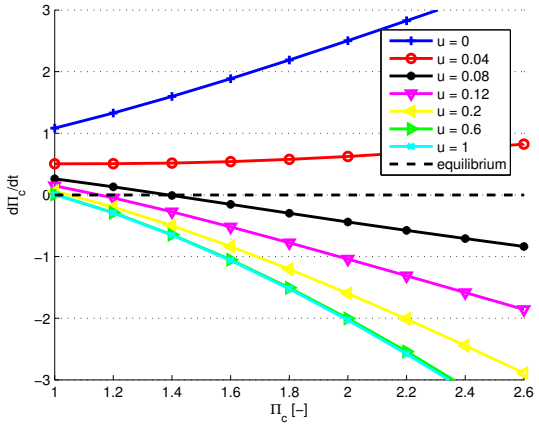

Fig. 2. $\dot{\Pi}_c$ as a function of Π_c, at 2000rpm.

It allows to look at the trajectories of the system when we consider a constant control input u. In Figure 2, we represent $\dot{\Pi}_c$ as a function of Π_c, at an engine speed of 2000 rpm, for different values of u. When the command is constant, the curves shown on the graph represent the trajectories of the system. The states of equilibrium correspond to the line $\dot{\Pi}_c = 0$ (the dotted line of Figure 2). When a curve crosses this line, the system state corresponds to an equilibrium point. Above this line, the state derivative is positive, and the state is increasing, so the system moves on its trajectory towards the right of the graph. Below the line, the state derivative is negative, and the system moves on its trajectory towards the left of the graph. As a consequence, if the trajectory is increasing with respect to Π_c, the equilibrium point is unstable, otherwise it is stable. On the other hand, if the curve does not cross the line $\dot{\Pi}_c = 0$, the system is unstable. At 2000 rpm, several behaviors are noticeable. First, when the wastegate is closed ($u = 0$), the curve is increasing while never crossing the equilibrium point. The system is unstable in this case with no equilibrium point. Moreover, when the wastegate is more open (u closer to 1), the system has stable equilibrium points.

C. Equilibrium states of the system

Since ψ_t is invertible (see [7]), system (1) is fully actuated and invertible. Thus, an analytic expression of the input can be derived from the state variables and their first derivatives. Indeed, from $(\Pi_c, \dot{\Pi}_c)$, we can compute

$$\Pi_t = \psi_t^{-1}\left(\frac{1}{\alpha_1}(\dot{\Pi}_c + \alpha_2\psi(\Pi_c))\right)$$

Then the input u can be computed using the static equality

$$u = \frac{\Pi_c - \alpha_3\phi_{turb}(\Pi_t)}{\alpha_3 S_{wg,max}\phi_{wg}(\Pi_t)}$$

The gathering of the two previous equations leads to an expression of u as a function of Π_c and $\dot{\Pi}_c$. This inverse model is noted g.

$$u = g(\Pi_c, \dot{\Pi}_c) \tag{2}$$

In the following, we also note g^{-1} the relation $\dot{\Pi}_c = g^{-1}(u, \Pi_c)$ obtained from the direct model (1).

The states of equilibrium of the system correspond to the solutions of a system of two equations with three variables ($\Pi_{c,eq}$, $\Pi_{t,eq}$, and u_{eq}). It corresponds to the inversion described above, with a state derivative equals to zero :

$$u_{eq} = g(\Pi_{c,eq}, 0) \tag{3}$$

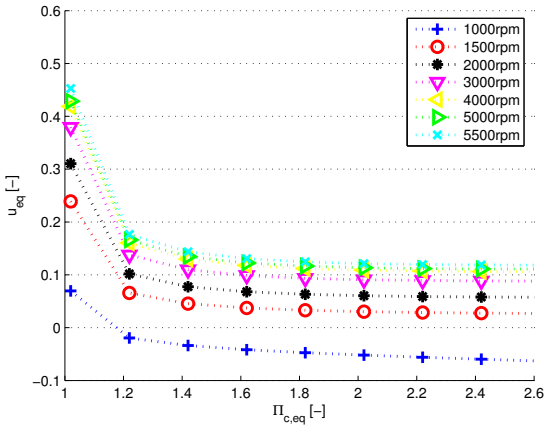

Fig. 3. States of equilibrium : u_{eq} as a function of $\Pi_{c,eq}$, for different engine speeds.

Figure 3 shows the different values of command u_{eq} depending on $\Pi_{c,eq}$, for different engine speeds. Since the command represents the section of the wastegate valve, negative values are not physically possible. At a given engine speed the maximum Π_c achievable corresponds to a command $u_{eq} = 0$. At 1000 rpm this value is lower than 1.2, whereas at higher speeds it is possible to reach 2.6, which is the limit allowed by the system.

From this analysis, it is also possible to compute the minimum input maintaining the pressure ratio at an equilibrium point lower than the maximum value allowed by the system, corresponding to a maximum turbocharger speed (set at a compression ratio of 2.6 in this case). Figure 4 shows this minimum command as a function of engine speed. At low engine speed the maximum pressure ratio can not be reached even with the actuator fully closed ($u = 0$).

D. Stability of the system

System (1) can be linearized around the states of equilibrium (defined by (3)) leading to the following representation (the command u_{eq} is considered constant) :

$$\left\{\begin{array}{rcl} \dot{x}_1 &=& a_1 x_2 - a_2 x_1 \\ x_1 &=& a_3 x_2 + a_4 u_{eq} x_2 \end{array}\right. \tag{4}$$

where $x_1 \triangleq \Pi_c - \Pi_{c,eq}$, $x_2 \triangleq \Pi_t - \Pi_{t,eq}$, and a_i are coefficients depending on the engine operating points :

$$\left\{\begin{array}{rclcrcl} a_1 &=& \alpha_1 \frac{d\psi_t}{d\Pi_t}(\Pi_{t,eq}) &,& a_2 &=& \alpha_2 \frac{d\psi_c}{d\Pi_c}(\Pi_{c,eq}) \\ a_3 &=& \alpha_3 \frac{d\phi_{turb}}{d\Pi_t}(\Pi_{t,eq}) &,& a_4 &=& \alpha_4 \frac{d\phi_{wg}}{d\Pi_t}(\Pi_{t,eq}) \end{array}\right.$$

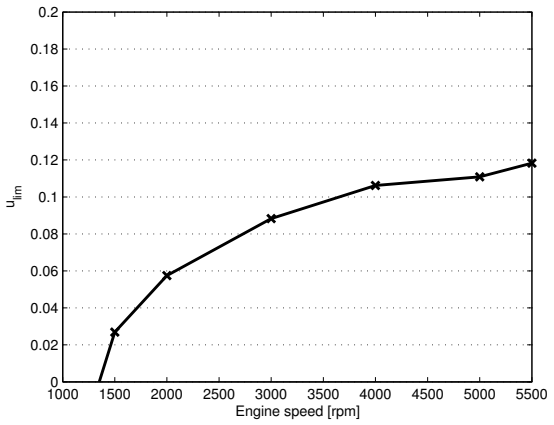

Fig. 4. Input limit to have a pressure ratio equilibrium less than 2.6 bar with respect to the engine speed.

System (4) can be rewritten as a first order linear system with a time constant depending of the constant input:

$$\dot{x}_1 = \tau(u_{eq})x_1 \quad \text{with} \quad \tau(u_{eq}) = \frac{a_1}{a_3 + a_4 u_{eq}} - a_2$$

The stability of the system around the equilibrium states is guaranteed if τ is negative. Figure 5 represents the value of τ as a function of $\Pi_{c,eq}$ for different engine speeds. It can be checked that τ remains always negative, and thus, all the equilibrium points are stable. However, τ is increasing : as the compressor ratio (and thus the engine load) increases, the system becomes closer to instability.

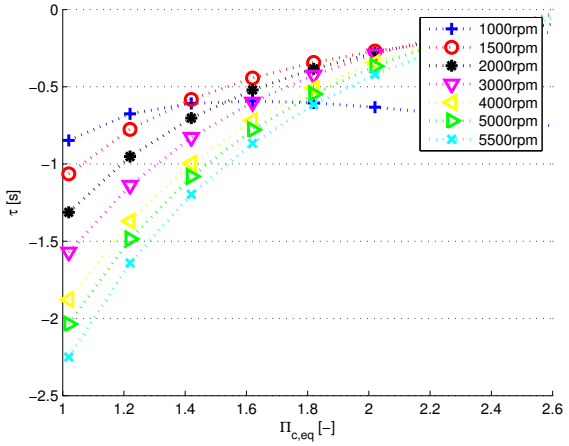

Fig. 5. States of equilibrium : $\tau(u_{eq})$ as a function of $\Pi_{c,eq}$, for different engine speeds.

E. Robustness

At this point of the analysis, it is interesting to consider the robustness of the stability of the system around the states of equilibrium. Since the coefficients α_i depend on environmental conditions and on systems characteristics that are known with an error margin, we can look at how a change in some parameters may affect the values of τ and hence the system stability. Figure 6 shows the values obtained when errors are added on the temperature upstream the turbine, and on the turbine efficiency, these values being considered as the more subject to an error. It can be noticed that the states of equilibrium remain stable.

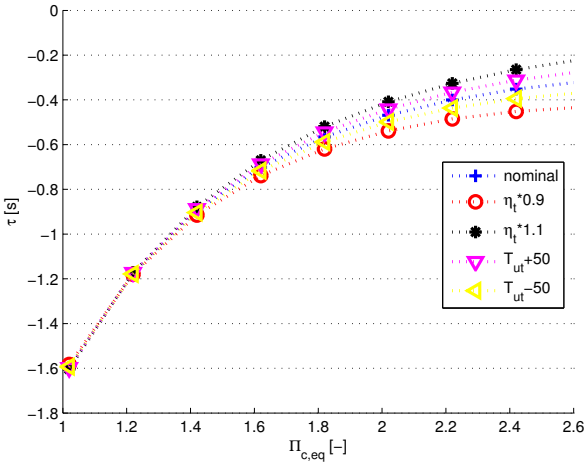

Fig. 6. Variation of τ for different errors introduced in the model, at an engine speed of 2000rpm.

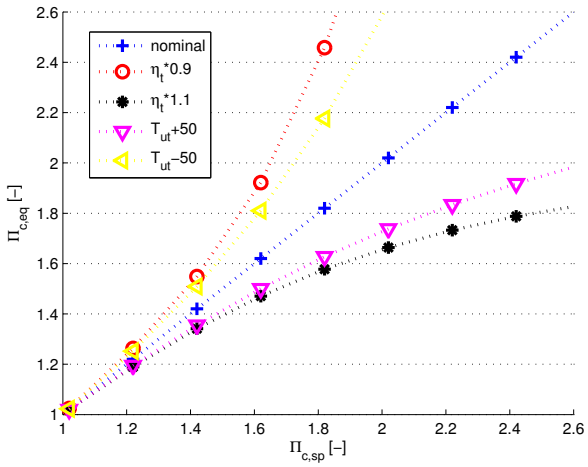

Fig. 7. Closed loop robustness for different errors introduced in the model, at an engine speed of 2000rpm.

Concerning the control strategy, the inversion (3) can be considered as a steady state feed forward term. For a desired pressure ratio set-point $\Pi_{c,sp}$, the steady state command u_{ss} is determined by $u_{ss} = g(\Pi_{c,sp}, 0)$. The behavior of the resulting closed loop system can be studied by applying this command to system (1) and computing the states of equilibrium obtained. A representation of the compression ratio $\Pi_{c,eq}$ for a desired $\Pi_{c,sp}$ shows the steady state error of the control strategy in Figure 7. The states of equilibrium are on the line $y = x$ when the model in the control law

matches perfectly the system, and deviates from this line when some errors are introduced in the model. Undesired behaviors appear at high compression ratios, when the state of equilibrium can be very different from the set-point. In some cases, the maximum compression ratio is higher than the maximum value allowed by the system. This lack of robustness of the closed loop system comprising only an inversion of the steady state part of the model as a feed forward underlines the necessity of a feedback term in the strategy.

V. Control strategy

A. Feedback design

The control strategy is directly obtained from the simplified model proposed above. We want the system to follow the dynamics described by :

$$\dot{y} = -\mu_p y \tag{5}$$

with $y = \Pi_{c,sp} - \Pi_c$

Using a similar approach as described in the previous section to compute a feed forward strategy, the closed loop command can be deduced from the model, ensuring a convergence to the desired set-point. An additional integral term is introduced in order to take account of modelling uncertainties.

$$\left\{ \begin{array}{rcl} u_{sp} & = & g(\Pi_{c,sp} + \mu_p(\Pi_{c,sp} - \Pi_c) + \mu_i z, \dot{\Pi}_{c,sp}) \\ \dot{z} & = & \Pi_{c,sp} - \Pi_c \end{array} \right. \tag{6}$$

The designed control strategy satisfies the requirements and constraints exposed in Section III :

- The manifold pressure is controlled to its set point.
- In steady state, the throttle is opened, minimizing the pressure drop across this component.
- The environment conditions are taken into account in the model.
- Since the speed of the turbocharger shaft is directly linked to the compressor pressure ratio, a limit on the set-point will ensure the safety of the system by maintaining the shaft speed below a maximum value.

B. Actuator Constraints and Anti Windup design

Control strategy (6) was already detailed in [7]. However, it does not take into account the constraints on the actuator. This can lead to undesirable behaviors, like integrator windup, potentially dangerous for the integrity system. The control strategy was therefore modified.

We note $sat(u, u_{min}, u_{max})$ the function defined by

$$sat(u, u_{min}, u_{max}) = \left\{ \begin{array}{lll} u_{min} & \text{if} & u \leq u_{min} \\ u & \text{if} & u_{min} \leq u \leq u_{max} \\ u_{max} & \text{if} & u_{max} \leq u \end{array} \right.$$

The first modification added to the strategy consisted in taking into account the actuator constraints for the computation of the trajectory set-point. The set-point derivative $\dot{\Pi}_{c,sp}$ is saturated so that it respects the limit on the command u. The saturated set-point, called $\Pi_{c,sat}$ is obtained from the filter defined by

$$\begin{array}{rcl} \dot{\Pi}_{c,sat} = & sat(\beta(\Pi_{c,sp} - \Pi_{c,sat}), \\ & g^{-1}(u_{max}, \Pi_{c,sat}), g^{-1}(u_{min}, \Pi_{c,sat})) \end{array} \tag{7}$$

where β is a gain tuning the dynamics of the filter.

The trajectory thus defined is feasible by the system. It ensures that the command u_{sp} computed by the control law $u_{sp} = g(\Pi_{c,sat}, \dot{\Pi}_{c,sat})$ respects the constraints $u_{sp} = sat(u_{sp}, u_{min}, u_{max})$. However, this is not true when model uncertainties are considered, neither with the complete control law defined by equation (6). An anti windup scheme is therefore designed. We used a similar approach as the one presented in [**?**] and detailed in [**?**] for the linear case. The integral term z in equation (6) is modified as below :

$$\left\{ \begin{array}{rcl} \dot{z} & = & \Pi_{c,sp} - \Pi_c - e\mu_{aw} z \\ \dot{w} & = & |u_{sp} - sat(u_{sp}, u_{min}, u_{max})| - w \\ e & = & sat(w, 0, 1) \end{array} \right. \tag{8}$$

The complete control law, considering actuator constraints and including an anti windup term is then defined by the system

$$\left\{ \begin{array}{rcl} \dot{\Pi}_{c,sat} & = & sat(\beta(\Pi_{c,sp} - \Pi_{c,sat}), g^{-1}(u_{max}), g^{-1}(u_{min})) \\ u_{sp} & = & g(\Pi_{c,sat} + \mu_p(\Pi_{c,sat} - \Pi_c) + \mu_i z, \dot{\Pi}_{c,sat}) \\ \dot{z} & = & \Pi_{c,sat} - \Pi_c - e\mu_{aw} z \\ u_{sat} & = & sat(u_{sp}, u_{min}, u_{max}) \\ \dot{w} & = & |u_{sp} - u_{sat}| - w \\ e & = & sat(w, 0, 1) \end{array} \right. \tag{9}$$

The command u_{sat} is applied to the system. This strategy corresponds to the sketch shown in Figure 8, where

- Σ represents the physical system.
- C represents the control law defined by equation (6).
- AW represents the anti windup scheme defined by (8).
- sat represents the setpoint filtering corresponding to the input limitation defined by equation (7).

VI. Experimental results

The results of an engine test stand are presented to portray the capabilities of this concept. The control was tested in transient consisting of engine load steps at fixed engine speed (2000 rpm). All unmeasured disturbances act upon the plant and the degrees of freedom (the parameters μ) were calibrated online on the engine test stand to set it for the actual disturbances. In this case calibration of μ were performed manually. Most model parameters were identified off-line using manufacturer data and additional measurements. The results presented here show the performance of the control strategy (9). It is compared with (6) which does not take into account the constraints on the actuator, and with the same strategy combined with the addition of the filter on the set-point (7), or with the addition of the anti windup scheme (8). The purpose of this approach is to emphasize the advantage of each part of the controller.

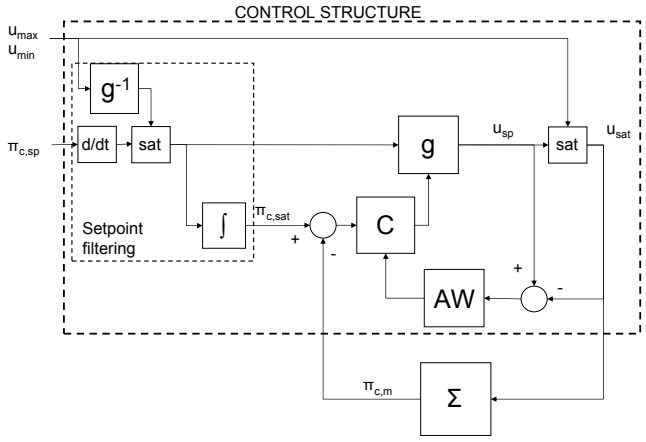

Fig. 8. Control strategy schematics.

A. Robustness: anti wind up strategies (AW)

Figure 9 shows the results obtained with an error introduced on the turbine efficiency (gain of 0.9), in order to study the robustness of the strategies. The upper graph represents the compression ratio Π_c, and the lower graph shows the command u_{sat}. The strategy is enabled at the time $t = 5s$ when the load step is applied. Before this time, the system is in open loop and shows a steady state error. The original strategy (6) (blue dashed-dot) exhibits an overshoot and a slow return to the set-point. Increasing the integral gain μ_i results in a faster convergence, but a much higher overshoot (red dashed). The complete strategy (9) (black solid) decreases the overshoot with the same integral gain, allowing a fast convergence to the set-point without any inconvenience due to the windup of the integral term during the transient when the command is saturated.

B. Anti windup and setpoint filtering (AW+sat)

The following figures 10 and 11 show a comparison between the control strategy (6) without any actuator constraints consideration, the strategy with filter (7) and the strategy with the anti windup (8). In figure 10, the value of Π_c presents similar features as the ones commented above : the strategy with no protection results in high overshoot whereas the two others allow to decrease the overshoot with a fast convergence. Figure 11 compares the different terms of the strategies. It can be seen that the integral term winds up if no consideration is taken for the actuator constraints, and that both the other strategies allow a reduction of this wind up. The main difference between the strategy with filter (7) and the strategy with anti windup (8) lies within the relative importance of the feed forward and feedback terms. The saturation of the set-point to a feasible trajectory results in a more important feed forward term, and less feedback. This behavior is very interesting when the model is accurate.

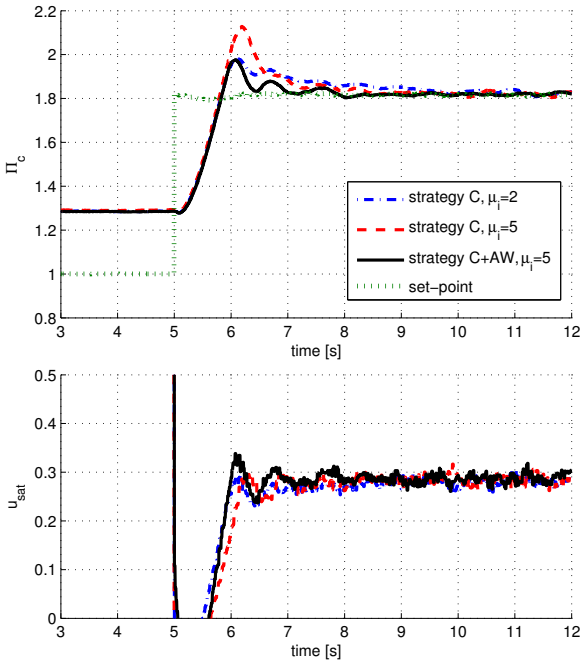

Fig. 9. Experimental pressure control. Load step at 2000rpm. Comparison between different control strategies with model errors. Controller C corresponds to the model based control defined by (6). The wind up strategy corresponds to equation (8).

VII. Conclusion

This paper describes the development of a model based control of a turbocharger in a gasoline engine. A first part proposes a thorough analysis of the system properties in terms of states of equilibrium, stability and robustness. A second part details the design of a control strategy, justified by the previous analysis. The actuators constraints are taken into account by a filter on the desired set-point, and an anti windup scheme is added in order to prevent undesired behaviors due to modelling uncertainties. The control strategy was validated experimentally, showing the relevance of the approach. The contributions of the different parts of the strategy are studied on experimental data.

Acknowledgments

The authors would like to thank Alexandre Chasse and Gilles Corde for valuable discussions that significantly contributed to this work.

References

[1] G. Colin, Y. Chamaillard, G. Bloch, and A. Charlet, "Exact and linearized neural predictive control: A turbocharged si engine example," *Journal of Dynamic Systems, Measurement, and Control*, vol. 129, no. 4, pp. 527–533, 2007.

[2] L. Eriksson, L. Nielsen, J. Brugard, J. Bergström, F. Pettersson, and P. Andersson, "Modeling of a turbocharged S.I. engine," *Annual Reviews in Control*, vol. 26, 2002.

[3] L. Eriksson, "Modeling and control of turbocharged SI and DI engines," *Oil & Gas Science and Technology - Rev. IFP*, vol. 62, no. 4, pp. 523–538, 2007.

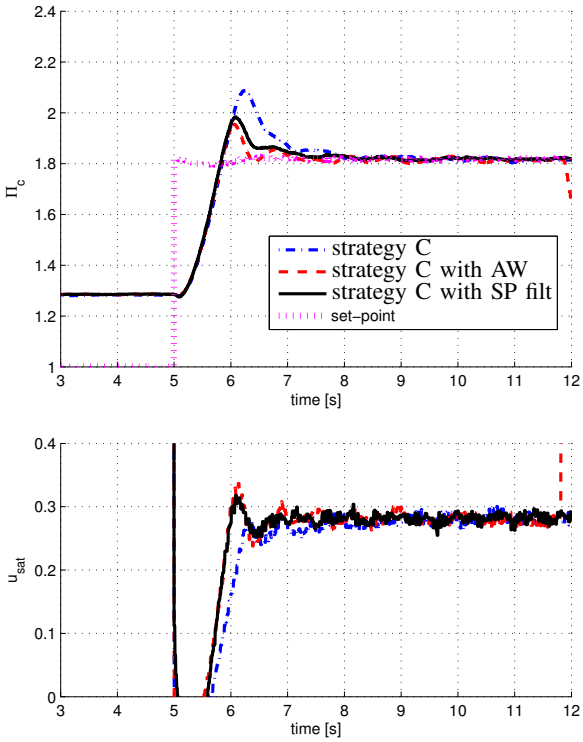

Fig. 10. Experimental pressure control. Load step at 2000rpm. Comparison between different control strategies. Controller C corresponds to the model based control defined by (6). The wind up strategy corresponds to equation (8). The set point filtering corresponds to the filtering (7).

[4] J. Jensen, A. Kristensen, S. Sorensen, N. Houbak, and E. Hendricks, "Mean value modeling of a small turbocharged Diesel engine," in *Proc. of the SAE Conference*, no. 910070, 1991.

[5] A. Karnik, J. Buckland, and J. Freundenberg, "Electronic throttle ans wastegate control for turbocharged gasoline engines," in *Proc. of the American Control Conference*, 2005.

[6] P. Moraal and I. Kolmanovsky, "Turbocharger modeling for automotive control applications," in *Proc. of the SAE Conference*, no. 1999-01-0908, 1999.

[7] P. Moulin, J. Chauvin, and B. Youssef, "Modelling and control of the air system of a turbocharged gasoline engine," in *Proc. of the IFAC World Conference*, 2008.

[8] S. Ouenou-Gamo, A. Rachid, and M. Ouladsine, "A nonlinear controller of a turbocharged diesel engine using sliding mode," in *Proc. of the Conf. on Control Application*, 1997.

[9] D. Schwarzmann, R. Nitsche, and J. Lunze, "Diesel boost pressure control using flatness-based internal model control," in *Proc. of the SAE Conference*, 2006.

[10] S. Sorenson, E. Hendricks, S. Magnusson, and A. Bertelsen, "Compact and accurate turbocharger modelling for engine control," in *Proc. of the SAE Conference*, 2005.

[11] R. Wakentan and D. Wright, "Closed loop turbocharger control with transient wastegate functions," in *Proc. of the SAE Conference*, no. 860487, 1986.

[12] B. Youssef, P. Moulin, and O. Grondin, "Model based control of turbochargers : Application to a diesel HCCI engine," in *Proc. of the Conf. on Control Application*, 2007.

[13] J. Zurlo, E. Reinbold, and J. MucHer, "The waukcsha tur bocharger control module: A tool for improved engine efficiency and response," in *Proc. of the ASME. Fall Technical conference*, 1996.

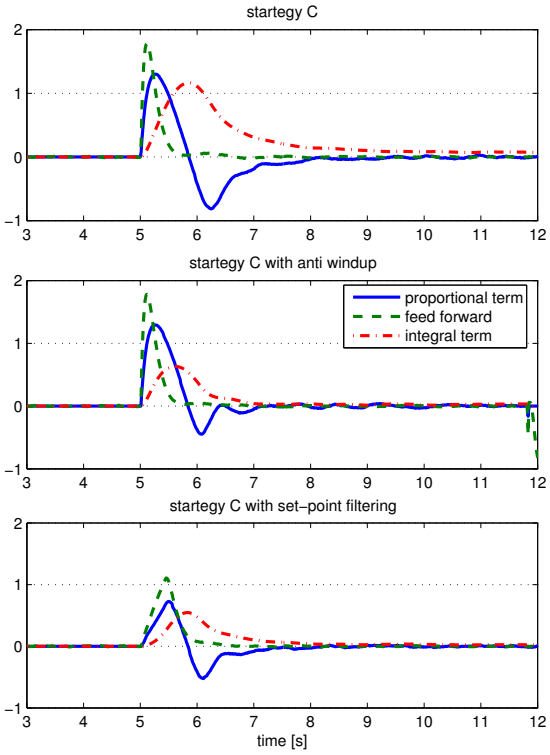

Fig. 11. Experimental pressure control. Load step at 2000rpm. Comparison between different control strategies and the contribution of each part of the control law. Controller C corresponds to the model based control defined by (6). The wind up strategy corresponds to equation (8). The set point filtering corresponds to the filtering (7).